

Inert Doublet Dark Matter and Mirror/Extra Families after Xenon100

Alejandra Melfo,^{1,2} Miha Nemevšek,^{2,3} Fabrizio Nesti,² Goran Senjanović,² and Yue Zhang^{2,*}

¹*Universidad de Los Andes, Mérida, Venezuela*

²*ICTP, Trieste, Italy*

³*J. Stefan Institute, Ljubljana, Slovenia*

(Dated: October 22, 2018)

It was shown recently that mirror fermions, naturally present in a number of directions for new physics, seem to require an inert scalar doublet in order to pass the electroweak precision tests. This provides a further motivation for considering the inert doublet as a dark matter candidate. Moreover, the presence of extra families enhances the Standard Model Higgs-nucleon coupling, which has crucial impact on the Higgs and dark matter searches. We study the limits on the inert dark matter mass in view of recent Xenon100 data. We find that the mass of the inert dark matter must lie in a very narrow window 75 ± 1 GeV while the Higgs must weigh more than 400 GeV. For the sake of completeness we discuss the cases with fewer extra families, where the possibility of a light Higgs boson opens up, enlarging the dark matter mass window to $\frac{1}{2}m_h - 76$ GeV. We find that Xenon100 constrains the DM-Higgs interaction, which in turn implies a lower bound on the monochromatic gamma-ray flux from DM annihilation in the galactic halo. For the mirror case, the predicted annihilation cross section lies a factor of 4-5 below the current limit set by Fermi LAT, thus providing a promising indirect detection signal.

PACS numbers: 14.65.Jk, 14.60.Hi, 14.80.Ec, 95.35.+d

I. INTRODUCTION

Recent data released by the Xenon collaboration [1], relative to 48000 kgd statistics, improve previous limits on the Dark Matter (DM) direct detection cross section versus the DM mass. This result has significant implications for scenarios of Dark Matter based on particle physics.

One popular such scenario, pursued in recent years, is the inert scalar doublet extension of the minimal Standard Model [2]. While its great virtue lies in its simplicity, the stability of the inert candidate is assumed without any theoretical hint in its favor.

As we argued in a recent paper [3], the inert nature of the second doublet is favored by electroweak precision tests (EWPT) constraints in the presence [4] of mirror families. Mirror fermions are a must in a number of physically motivated scenarios: Kaluza-Klein theories [5], family unification based on large orthogonal groups [6–8], $N=2$ supersymmetry [9] and some unified models of gravity [10]. Moreover, they were envisioned by Lee and Yang in their classic paper on parity breakdown [11] as a way to restore parity in the fundamental interactions.

Such a framework becomes quite predictive when constraints from the EWPT and the vacuum stability of the Higgs potential [3] are considered. The lowest component of the inert doublet, which is a possible dark matter candidate, must have a mass less than around 100 GeV.

In view of this, we study the dark matter direct detection in the presence of three extra chiral mirror families, taking into account the recent data from the Xenon100 experiment. The key point here is the enhancement of the effective Higgs portal to the nucleon in the presence

of the extra heavy fermions [12]. This is precisely the same diagram which enhances the Higgs production cross section at hadron colliders. In the presence of mirror families the enhancement of direct detection gives approximately a factor of 9, so with the new Xenon100 bound this scenario becomes predictive for the mass and possible annihilation channels of the inert dark matter. In turn, this framework predicts a lower bound on the monochromatic gamma ray line from the annihilation in the galactic halo, whose cross section is less than an order of magnitude below the current Fermi LAT sensitivity.

It is important to keep in mind that although the mirror case provides a good rationale for the stability of the inert DM candidate, generically it may not be necessary to stick to the mirror conjecture. In fact, none of the results we present depend on the choice of chirality of the extra fermions, and as such they are equally applicable to the usual additional copies of the SM families. In what follows, we present our results for one to three extra families (more are not allowed by precision tests) in the presence of an extra inert doublet.

The paper is organized as follows. In the section II, we describe the theoretical and experimental constraints on the inert doublet extension of the SM with extra families. We include the limits from direct collider searches, the electroweak precision constraints, perturbativity and vacuum stability, and describe the updated Tevatron Higgs exclusion window in this model. In Section III, we present our results for the relic density and direct detection, which constrain the DM mass to lie between $\frac{1}{2}m_h - 76$ GeV for a fourth family and in a very narrow window 75 ± 1 GeV in the case of the three mirror families. This enables us to give a quite robust prediction for the monochromatic gamma ray flux from the galactic halo. Section IV contains a summary and the outlook.

* amelfo@ictp.it, miha@ictp.it, goran@ictp.it, nesti@aquila.infn.it, yuezhang@ictp.it

II. EXTRA/MIRROR FAMILIES SEEKING FRIENDSHIP WITH AN INERT DOUBLET

As we will describe now, the EWPT together with the constraints from perturbativity and vacuum stability, favor the existence and inertness of an extra doublet, Φ . After the electroweak symmetry breaking, this field decomposes into an extra scalar S , a pseudoscalar A and a charged component C .

A. Vacuum stability and perturbativity

The large Yukawa couplings of the extra quarks become a problem for vacuum stability in the case of a light SM Higgs, as they tend to drive the Higgs boson self coupling to negative values. Therefore, one should take the extra quarks as light as possible, without running into conflict with direct search, ~ 350 GeV. Still, in the case of more than one extra family, the light Higgs mass window $115 \text{ GeV} \lesssim m_h \lesssim 131 \text{ GeV}$ is excluded if the vacuum is to be stable up to a reasonably high cut-off (e.g. 1 TeV). In particular with three extra families (mirror case), the SM Higgs boson needs to be heavier than ~ 400 GeV [3]. At the same time the requirement of perturbativity imposes an upper bound on the SM Higgs mass, which is about 600 GeV [2, 15], as well as on the mass (Yukawa couplings) of heavy fermions, which have to be lighter than roughly 500 GeV. All this has important implications for the discussions of the EWPT, in the next section (see Fig. 1).

Concerning the components of the extra doublet, in the mass ranges that are favored by EWPT, they have no appreciable impact on perturbativity or/and stability of the SM Higgs.

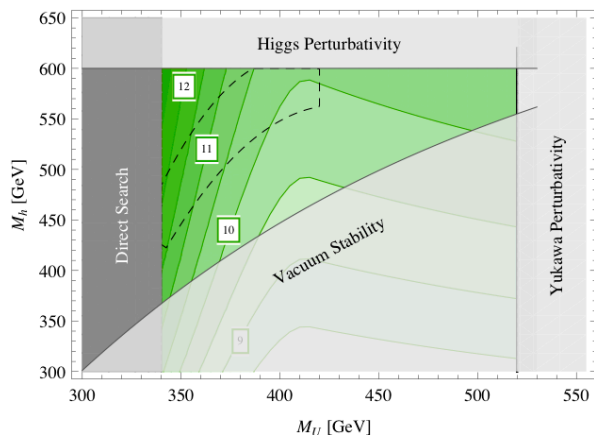


FIG. 1. Stability and perturbativity limits on m_h , m_U (shaded gray regions), in the presence of three extra generations. The central allowed region corresponds to a low cut-off $\Lambda = 700$ GeV; the dashed-contour region to $\Lambda = 1$ TeV. In the background, we report the χ^2 contours from Fig. 3, fourth panel, showing that the best points, with reasonably high cut-off, lie around $m_U \sim 400$ GeV and $m_h \sim 500$ GeV.

B. Electroweak Oblique Corrections

It has been shown in [4, 13] that with a fourth family one can fit the electroweak oblique parameters S , T , U to within 68% confidence level (CL). However, this becomes progressively constrained as more families are added, until $\chi^2 \approx 13.5$ for the case with three extra families, outside 99% CL.

The introduction of the second doublet can help to alleviate the tension (in appendix A we list the relevant expressions for its contribution). In fact, we have explored the best fit cases and find that they are characterized by a significant cancellation of the contributions to T from the (three) extra families and the doublet. In this case we find the best $\chi^2 \approx 9.0$, lying inside the 99% ellipse.

Qualitatively, one can understand what happens for the mirror case in the following way: Naively for heavy electroweak doublet fermions, the contribution to the S parameter is $1/(6\pi)$. Therefore, three extra families contribute around 0.7. However, as noticed recently [14], this relatively large contribution can be reduced by making the extra neutrinos lighter than the Z -boson. The T parameter receives a large positive contribution by splitting the extra neutrinos and charged leptons, which can be compensated by splitting the components of the second Higgs doublet. Finally, the reason one cannot get even an even better fit is due to the relatively large contribution in the U direction, again from splitting the lepton doublets of the extra families.

Fig. 2 illustrates the effect of adding an inert doublet and mirror families on the oblique parameters S , T and U . We show a projection in the $S - U$ plane of the 68%, 95% and 99% contours from [13], together with the value obtained for a heavy SM Higgs and how it changes with the addition first of an extra inert doublet, and then three extra families. Sample points are

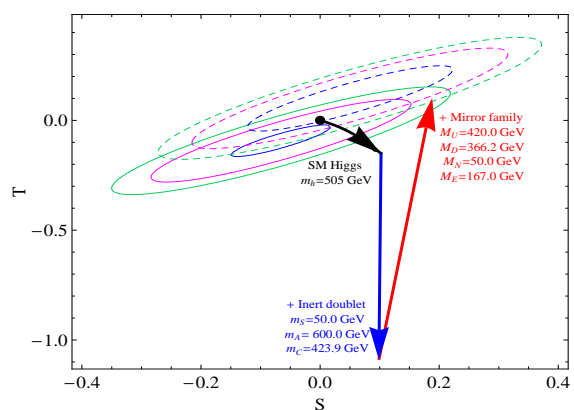


FIG. 2. An illustration of best fit point for the electroweak oblique corrections (the $S - U$ plane) with inert Higgs doublet and extra families. The contributions from SM Higgs, second doublet and mirror fermions are added in order. The best fit is associated with a large cancellation in the T direction. The arrows starts from the reference plane where $U = 0$ (dashed) and end up on the plane with $U = 0.269$ (continuous).

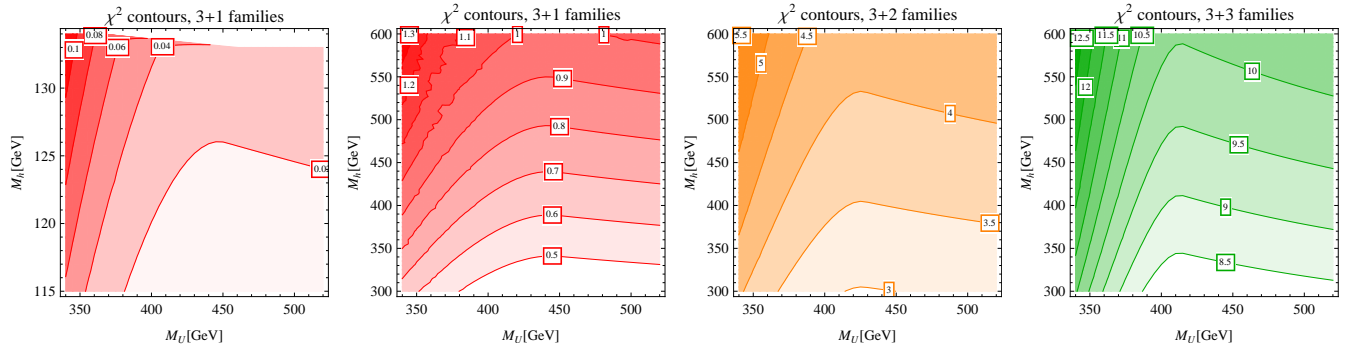


FIG. 3. The best χ^2 contour in the m_h - m_U parameter space, for one, two and three extra families with a second doublet. For one extra family, the SM Higgs can be either light or heavy (first and second panel) while for the case with more families, the vacuum stability constrains the Higgs to be heavy.

given for a set of fermion and scalar masses that provide the best fit: $m_h = 505.0$ GeV, $m_S = 50.0$ GeV, $m_C = 423.9$ GeV, $m_A = 600.0$ GeV, and $m_U = 420.0$ GeV, $m_D = 366.2$ GeV, $m_N = 50.0$ GeV, $m_E = 167.0$ GeV.

In Fig. 3 we show, for one to three extra families, the contours of the best χ^2 in the m_h - m_U parameter space. Other mass parameters are varied in the range consistent with direct search limits (see Table I below) in order to optimize the fit, and we have taken into account the lower bound on the SM Higgs mass due to vacuum stability. Indeed, for a fourth family the Higgs can be either light ($m_h \in [114, 131]$ GeV) or heavy ($m_h > 204$ GeV). For more families instead, the vacuum stability bound becomes relevant: $m_h \gtrsim 300$ GeV and $m_h \gtrsim 400$ GeV for two and three extra families, respectively. The results, shown in Fig. 3, can be summarized as follows:

- The best fits are obtained when Higgs is lighter.
- For one and two extra families one can always find solutions so that the oblique parameters are fit to within 68% CL.
- In contrast, for three extra families, the SM Higgs is constrained to be heavier than 400 GeV, so that the best χ^2 turns out to be much higher, see Fig. 1, where we bring together the EWPT and vacuum stability and perturbativity constraints.

It turns out that for the mirror case the best fit scenario is very predictive regarding the mass spectrum. First, the extra charged leptons and (especially) neutrinos are constrained to be light, while the quarks have to lie around 400 GeV and the Higgs around 500 GeV to be safe from vacuum instability (see Fig. 1). Then, the scalars from the second doublet are constrained to lie in the range 250 GeV $\lesssim m_C \lesssim 500$ GeV and $m_A \gtrsim 450$ GeV. Also, at the best fit point, the scalar component S has to be lighter than 100 GeV. This is only possible if S has tiny (or no) mixing with the SM Higgs boson, to avoid the LEP bound on Higgs-like particles. Finally, the χ^2 is also minimized when the extra doublet does not mix at all with the standard Higgs one [3].

C. An inert doublet

The fact that the inert nature is favored by EWPT provides a motivation to take the lightest neutral component in the second doublet to be the dark matter candidate. Before pursuing such possibility in detail, we will define the potential and study the relevant experimental bounds on the Higgs sector.

In this scenario, the extra scalar doublet does not develop a vacuum expectation value and is not coupled to fermions [2, 15, 16]. Assuming the stability of its lightest member implies an exact Z_2 symmetry,¹ which restricts the potential to the following form:

$$V = \mu_1^2 |H|^2 + \mu_2^2 |\Phi|^2 + \lambda_1 |H|^4 + \lambda_2 |\Phi|^4 + \lambda_3 |H|^2 |\Phi|^2 + \lambda_4 |H^\dagger \Phi|^2 + \frac{\lambda_5}{2} ((H^\dagger \Phi)^2 + \text{h.c.}). \quad (1)$$

Clearly, all terms are odd under the Z_2 symmetry.

Experimental bounds on the inert doublet scalars and extra leptons derive mainly from LEP, while the extra quarks are required to be very heavy from direct searches at the Tevatron and LHC. We summarize the bounds on new fermions and inert scalars in Table I, and refer the reader for details to [3] and references therein.

LEP	$m_N > 45$ GeV , $m_E > 102.6$ GeV $m_C > 70$ GeV, $m_S > 50$ GeV, $m_S + m_A > M_Z$
CDF	$m_U > m_D > 335$ GeV , $m_D > m_U > 338$ GeV
CMS	$m_D > 361$ GeV

TABLE I. Experimental bounds on extra fermion and inert doublet components, used for the fitting.

¹ Strictly speaking, this symmetry need only be approximate as long as the DM candidate is sufficiently long-lived. We discuss this issue in section III.C.

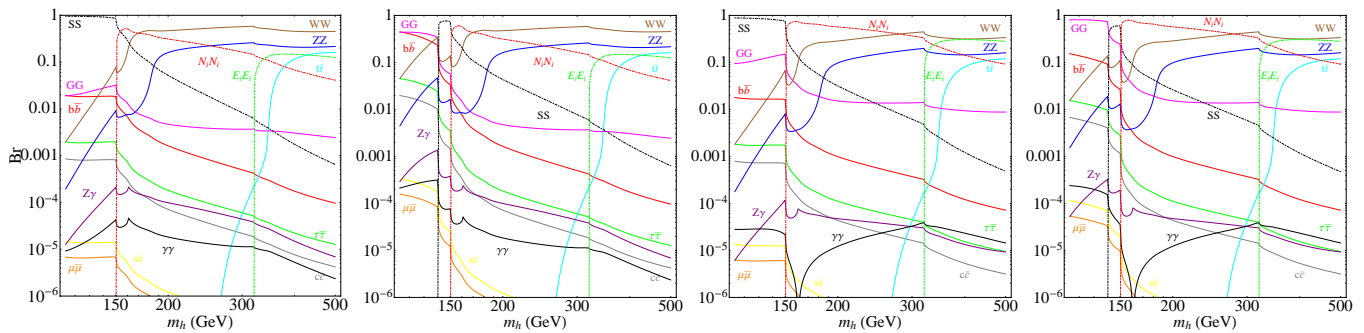


FIG. 4. Branching ratios of SM Higgs boson in the inert doublet model with a fourth family (first and second panels) and three extra or equivalently mirror families (third and fourth). In the plot, we have taken $m_S = 50$ GeV (first, third) and 70 GeV (second, fourth), $m_{N_i} = 75$ GeV, $m_{E_i} = 160$ GeV, $m_{U_i} = m_{D_i} = 350$ GeV, $m_C = 450$ GeV and $\lambda_L = 0.3$.

D. Implications on the SM Higgs search

An extension with a second Higgs doublet and extra families changes both the production and decays of the SM Higgs boson. We calculate the branching ratios using HDECAY [17] as shown in Fig. 4, with possible new decay channels into SS , $N\bar{N}$ and $E\bar{E}$. Meanwhile, the existence of extra quarks will enhance $H \rightarrow gg$, which dominates the branching ratios before the SS decay channel opens. Both extra quarks and leptons contribute destructively [18] with the W -boson to the branching ratio $H \rightarrow \gamma\gamma$. We find such destructive interference is most complete for two extra families. For one or three extra families, the suppressions of diphoton branching ratio are similar, about 0.01 – 0.1 of the SM value, for a light Higgs. We also noticed the charged scalar C from the inert doublet makes a negligible contribution [19] to the $H \rightarrow \gamma\gamma$ branching ratio.

On the other hand, the Higgs production cross section via gluon fusion also receives enhancement due to the presence of heavy chiral quarks. Combining these effects, we use the most recent results on Higgs searches from D0 and CDF [22] to evaluate the exclusion window on the Higgs boson mass. With the presence of a fourth family, the enhancement factor is roughly a factor of 9, for $m_h < 200$ GeV. This has been used by [22] to claim the exclusion region between 131 – 204 GeV.²

However, this does not hold for light extra neutrino N as argued in [24], because the Higgs “invisible” decay significantly reduces the branching ratio of WW channel used for the identification of the Higgs. Similarly, if the scalar S is sufficiently light (even for heavy N), i.e., $m_S \approx 50$ GeV, the Tevatron exclusion window on the Higgs boson mass shrinks to ~ 150 – 200 GeV. At the same time, the $H \rightarrow SS$ channel dominates for all the light Higgs mass values, as can be seen in Fig. 4. In any case, there is still the bound from the LEP: $m_h \gtrsim 114$ GeV [20].

For the mirror families case, the Higgs production cross

section gets enhanced 49 times for $m_h < 200$ GeV [20] and this factor gets reduced to as much as ~ 20 for heavier Higgs near the $t\bar{t}$ threshold [21]. In this case, the Tevatron direct search excludes the Higgs mass window between ~ 160 – 250 GeV for a light $m_S \approx 50$ GeV and moderate $\lambda_L \approx 0.3$. Taking a slightly heavier $m_S \approx 70$ GeV, the exclusion window will extend to ~ 130 – 250 GeV. It is useful to recall though, that vacuum stability with mirror families excludes the light Higgs regime anyway, and further imposes the lower bound $m_h \gtrsim 400$ GeV (Fig. 1).

III. INERT DOUBLET AS DARK MATTER

As a convention, we take S to be the lightest component of Φ and therefore the DM candidate (assuming A to be DM is physically equivalent, since a simple redefinition interchanges them). Of course, if extra families are included, the new neutrinos are available as an additional component of DM. This depends on the nature and mass spectrum of neutrino masses. In case they are Dirac particles, their contribution to the relic density is negligibly small, less than 0.3%. An appreciable contribution can be obtained by a judicious choice of their Majorana masses [24].³ We do not pursue this option here, so that S from the inert doublet by itself accounts for the DM.

The relevant interactions of S which govern the relic density and the direct detection are its interactions with W and Z , fixed by the gauge group representation and the following interaction with the SM Higgs boson:

$$\frac{\lambda_L v}{2} S^2 h, \quad \lambda_L = \lambda_3 + \lambda_4 + \lambda_5. \quad (2)$$

Throughout the analysis, we will take $m_A = m_C \approx 450$ GeV, a consequence of strong hierarchy between A , C and S , demanded in the case of three/mirror extra families. Therefore, the co-annihilation effects are safely neglected.

² For critical comments about the uncertainties in this result, see [23].

³ See also [25] for fourth generation RH neutrino being the DM candidate.

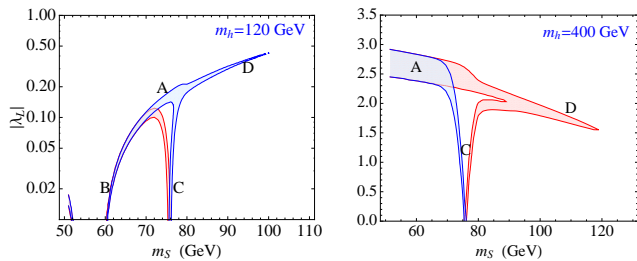


FIG. 5. WMAP allowed parameter space in the λ_L - m_S plane, for $M_h = 120$ (left) and $M_h = 400$ (right). The labels of regions refer to: $SS \rightarrow b\bar{b}$ away from the Higgs mass pole (A); $SS \rightarrow b\bar{b}$ on the Higgs mass pole (B); $SS \rightarrow WW$ near the threshold (C) and $SS \rightarrow WW$ for larger m_S (D). The red and blue colors stand for positive and negative λ_L , respectively.

A. Relic Density

To determine the relic density, we employ the `MicrOMEGAs` package [26], which includes all the relevant two body annihilation final states. The relic density is constrained by the WMAP five year data [27] to be $0.092 < \Omega h^2 < 0.128$, where Ω is the dark matter density and h is the normalized Hubble expansion rate.

The main processes controlling the thermal freeze-out of dark matter include the usual annihilation to weak gauge bosons, as well as the annihilation through the SM Higgs boson into $f\bar{f}$ (predominantly $b\bar{b}$) [16]. Thus, the relic density of the dark matter depends not only on m_S , but also on m_h and λ_L . Roughly, the viable parameter space can be divided into the following relevant regions which are depicted in Fig. 5.

- First, $SS \rightarrow h^* \rightarrow b\bar{b}$ (denoted A in Fig. 5) dominates the annihilations. This can happen for a light $m_S < 75$ GeV (this is when the WW channel takes over) and large enough λ_L/m_h^2 . Alternatively, the same happens for smaller λ_L/m_h^2 but when the center of mass energy is near the Higgs pole (denoted B in Fig. 5). The latter case corresponds to $m_S \approx \frac{1}{2}m_h$, as long as $m_h < 150$ GeV.
- Second, $SS \rightarrow WW$ dominates. This can happen either predominantly through the direct $SSWW$ coupling (denoted C), in which case in order to give the correct relic density m_S is forced to lie around 75 GeV; or through both the direct and Higgs mediated $SSWW$ couplings (denoted D). In this case, for proper values of λ_L/m_h^2 , one may obtain the correct relic density through judicious cancellation of the two contributions [28] and the mass of S extends from 75 to ~ 110 GeV.

In principle, the two body final state can be considered just as a subset of a more general annihilation channel $SS \rightarrow WW^*$. As was noticed in [29], the three body process becomes more relevant for $m_S \lesssim 75$ GeV, when

$SS \rightarrow b\bar{b}$ annihilation rate is low. The three-body annihilations have not yet been included in `MicrOMEGAs`, therefore the relic density $\Omega' h^2$ provided by `MicrOMEGAs` has to be rescaled to properly account for such an effect. In practice, we calculate the thermally averaged annihilation cross sections for both $SS \rightarrow WW$ and $SS \rightarrow WW^*$. Then, the correct relic density Ωh^2 is suppressed by the factor

$$r = \frac{\Omega}{\Omega'} = \frac{\langle \sigma v \rangle_{SS \rightarrow b\bar{b}} + \langle \sigma v \rangle_{SS \rightarrow WW}}{\langle \sigma v \rangle_{SS \rightarrow b\bar{b}} + \langle \sigma v \rangle_{SS \rightarrow WW^*}}, \quad (3)$$

where the thermally averaged cross sections are evaluated at $T_f = m_S/25$.

It is useful to note that the branching ratios depicted in Fig. 4 help to properly determine the SM Higgs propagator when the annihilation happens at the resonance.

An important point to note is the possibility of annihilation of S into neutrinos from extra families, which have large couplings to the Higgs boson. If such an annihilation channel is open, because of the large Yukawa couplings of N , the SSh coupling must be dramatically reduced in order to keep the relic density intact. In this case, the direct detection cross section is accordingly reduced, and will typically end up being below the Xenon sensitivity. There is also an intermediate scenario with m_N just slightly below m_S , where the direct detection may still be possible. We will comment on this possibility below. Let us first focus on the scenario where all the extra neutrinos are heavier than S .

B. Direct Detection with Extra Families

Direct detection of the inert dark matter is mediated by the exchange of the SM Higgs boson with nucleons at tree level [12]. The effective matrix element for the Higgs interaction with the nucleon is [31],

$$\frac{1}{v} \langle N | \sum_q m_q \bar{q}q | N \rangle = \frac{m_N}{v} f(n_h),$$

$$f(n_h) = \left(1 + \frac{2n_h}{27} \right) (f_{T_u}^{(N)} + f_{T_d}^{(N)} + f_{T_s}^{(N)}) + \frac{2n_h}{27}, \quad (4)$$

where the sum over q goes through all the quarks, m_N is the nucleon mass, n_h is the number of heavy quarks and $\langle N | m_q \bar{q}q | N \rangle \equiv m_N f_{T_q}^{(N)}$ is the nucleon sigma term for light flavors. Clearly, the strength of the effective interaction depends on the number of heavy quarks, which contributes democratically. In the following analysis, we use the central values of f_{T_q} in [31] from the lattice results and get $f(n_h = 3) = 0.375$ for the SM which is close to the central value used in [30].⁴ The extra family extension will boost such interactions, yielding $f(5) = 0.542$

⁴ Our conclusions remain the same if a relatively higher value of $f = 0.467$ is used, as in the `MicrOMEGAs` package. In order to be as conservative as possible, a lower value of f is used throughout the paper.

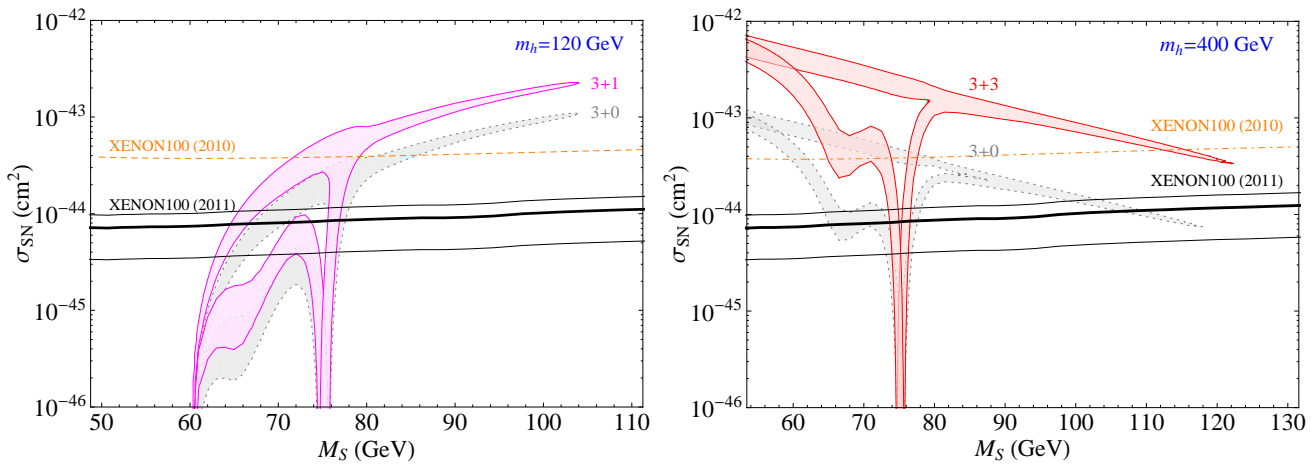


FIG. 6. Direct detection cross section on nucleon consistent with WMAP relic density region. Left Panel: light SM Higgs regime, $m_h = 120$ GeV, with one (solid region) and zero (dotted region) extra families. Right panel: heavy SM Higgs regime, $m_h = 400$ GeV with three (solid region) and zero (dotted region) extra families. The horizontal solid lines show the Xenon100 limits for different local dark matter densities, $\rho_\odot = 0.2, 0.3, 0.6$ GeV/cm³ (upper to lower solid lines). The dashed line shows the limit from the previous (2010) Xenon data release.

for fourth family case and $f(9) = 0.875$ for three extra families. The main uncertainty in the matrix element comes from the strange quark contribution [32]. The direct detection cross section is thus

$$\sigma_{SN} = \frac{\lambda_L^2 f(n_h)^2}{4\pi} \frac{\mu^2 m_N^2}{m_h^4 m_S^2}, \quad (5)$$

where $\mu = m_S m_N / (m_S + m_N)$. In the case of mirror families there are 6 new heavy quarks and the direct detection cross section gets enhanced by a factor of 9. This facilitates the direct detection of this dark matter candidate.

It is then important to compare these predictions with the bound resulting from the recent Xenon100 released data [1]. For a realistic comparison, one has to also take into consideration the large uncertainty in the local DM density ρ_\odot . This quantity, which is necessary in converting the Xenon expected rate to the excluded cross section, is inferred only from very indirect and uncertain measurements, and can at best be constrained to lie in the fairly broad range $\rho_\odot = 0.4 \pm 0.2$ GeV/cm³ [33]. This uncertainty then shifts the bound on the cross section, and is of relevance for the model under consideration.

In Fig. 6 we present the results of the comparison, for 3+1 families (left plot) which favors light Higgs and 3+3 families (right plot) which favors a heavy Higgs boson. These represents the main results of our work. As it can be seen, the upper bound set by Xenon100 narrows down the allowed region for the m_S , even in the hypothesis of low DM density, to one or two fixed values of m_h .

- Focusing first on the 3 + 1 case, if the SM Higgs is light, the DM mass is practically fixed by the legs of the “giraffe”. For example, for $m_h = 120$ GeV, the mass lies in the window between $\frac{1}{2}m_h$ and 76 GeV.

The former value corresponds to the annihilation through the SM Higgs boson to $b\bar{b}$ final states (with minor corrections from WW^*). The second value corresponds to annihilations to WW . On the other hand, when the SM Higgs is heavy, the DM mass is confined to a particular value around 75 GeV.

- The 3 + 3 case is represented by the red region in the right panel of Fig. 6. The allowed region has only one “leg”, because the Higgs has to be heavier than 400 GeV (for vacuum stability). Therefore, m_S must lie very near 75 GeV. Note that this value is only due to the WW annihilation channel and thus it is independent from the Higgs mass. Actually, the exclusion of the rightmost part (in contrary to zero extra family case) is quite insensitive to the particular choice of Higgs mass (as explained for case D in figure 5).

The Xenon collaboration also claimed a mild positive evidence of dark matter, whose cross section is just below the current bound. If true, it can be easily accommodated for the values of m_S discussed above.

Let us finally comment on the other possible scenario mentioned above, where some of the heavy neutrinos are lighter than S , allowing the annihilation $SS \rightarrow NN$. In this case, to maintain the correct relic density, the hSS coupling λ_L is reduced by a factor of at most $\sim 1/10$ and the direct detection regions shown in Fig. 6 are shifted downwards by 10^{-2} . This reduces the predictivity of this scenario in terms of the S mass, but implies in turn that m_N lies in a narrow region, $[45 \text{ GeV}, m_S]$, which is important for the detection of N at colliders. From the point of view of EWPT, both scenarios with either lighter or heavier than N are equally allowed.

C. Indirect Detection with Gamma-ray Line

As we saw above, the 100 live-day Xenon100 results restrict the DM mass to a narrow region, especially in the presence of mirror families. The main annihilation channel during freeze-out is to gauge bosons, while today in the galactic halo since the temperature is low, the annihilation through the SM Higgs to $b\bar{b}$ could be important. A spectacular signature of the inert doublet DM would be the observation of a monochromatic gamma-ray line from its annihilation in our galactic halo. This could serve as a promising signal of indirect detection to determine the mass of the DM. In this model, such process goes through a dimension six operator $SSF_{\mu\nu}F^{\mu\nu}$ with a loop suppression (mainly W -loop). The DM initial states SS can either couple to the W -loop directly, or through the SM Higgs to both W and heavy fermion loops. In fact, the associated loop functions are the same as those in the $h \rightarrow \gamma\gamma$ process. The implication of Xenon100 is the suppression of the SSH coupling and thus the Higgs mediated annihilation to two photon, which eliminates the possibility of any destructive cancellation. Therefore, there is a robust prediction of a lower bound on the gamma-ray line flux.

The Fermi LAT experiment has put constraints on the DM annihilation into gamma-ray lines between the energy 30–200 GeV [35]. In Fig. 7, we show the cross section as a function of the DM mass for $m_h = 400$ GeV and different values of λ_L , as well as the experimental bound assuming different halo density functions. For the mirror case where the DM mass is restricted to 74–76 GeV by WMAP and Xenon100, we find the predicted annihilation cross section $\sigma v(SS \rightarrow \gamma\gamma)$ lies only a factor of 4–5 below the current Fermi LAT bound. If the future data release can further push the limit down by one order of magnitude, one will be able to verify or exclude the possibility of the inert doublet being the DM candidate.

Decaying DM: approximate Z_2 symmetry? Up to now, as in previous studies we have assumed the dark matter to be absolutely stable. If it were to be so, it would imply the existence of an exact Z_2 symmetry. Observationally, dark matter does not have to be absolutely stable, and therefore one should be open minded to consider the possibility that the Z_2 symmetry is only approximate. The point is, that approximate global symmetries are equally useful in guaranteeing the naturalness of small couplings as the unbroken one. This is the essential criterion of naturalness. Needless to say, an unstable DM still has to be cosmologically long lived. A decaying scalar dark matter could also lead to mono-chromatic gamma-rays carrying energy equal to half of its mass. This process could go through the effective dimension five operator $(\epsilon/v)SF^{\mu\nu}F_{\mu\nu}$, where ϵ breaks the Z_2 symmetry explicitly. Fermi LAT imposes a stringent upper bound $\epsilon \lesssim 10^{-26}$.

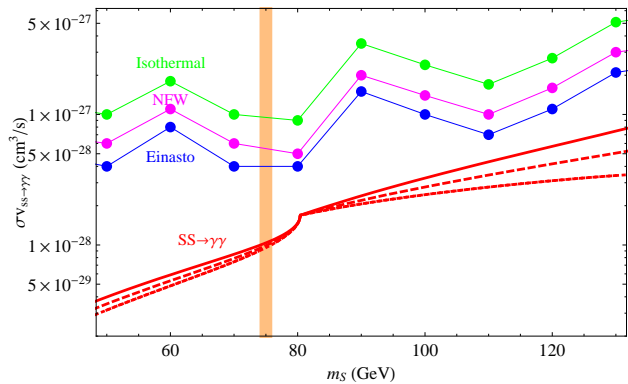


FIG. 7. Model prediction (red curves) and Fermi LAT constraints (blue, magenta, green) assuming different DM halo density distributions on the DM annihilation cross section to two monochromatic photons in the galaxy. We have taken $m_h = 400$ GeV. The solid, dashed, dotted curves correspond to $\lambda_L = -0.5, 0.01, 0.5$ respectively. The orange shaded region is the range of DM mass consistent with relic density and direct detection.

IV. LHC PROSPECTS

Finally, we comment on the LHC prospect of discovering or falsifying this theoretical setup.

Heavy quark states. The most obvious way to verify or falsify the above framework is to search the heavy quarks from extra families. Being colored states, they have large cross sections at hadron colliders. As mentioned in Sec. II, the current limits on the heavy quarks are around 350 GeV, mainly from Tevatron. With higher energy and luminosity, LHC can soon push the mass limits into the non-perturbative regime, where new bound states could emerge whose properties largely depend on the corresponding Yukawa couplings [36].

Inert dark matter signatures. The signatures of the inert doublet model have been studied in [37, 38], focusing on the multi-lepton final states. One should keep in mind that a typical mass spectrum of the inert doublet is quite hierarchical in the mirror scenario under consideration. In particular, we find A to be the heaviest inert scalar $450 \text{ GeV} < M_A < 600 \text{ GeV}$, the mass of C lies in the intermediate range $250 \text{ GeV} < m_C < 500 \text{ GeV}$ and S is very light $50 \text{ GeV} < m_S < 150 \text{ GeV}$. The resulting signatures after their pair production at the LHC differ slightly from the previous analyses, due to the large mass hierarchy and potential cascade decays of both A and C . Therefore, the final state leptons and jets possess large transverse momentum. Meanwhile, due to the fact that any such final state always contains a pair of S , the resulting missing energy will also be typically larger than 100 GeV. These characteristics can be fully tested when the energy of LHC reaches 14 TeV.

Are mirror neutrinos Majorana? A priori, just as in the SM, we cannot know the nature of neutrinos. The

dominant view today is the Majorana picture which, if true, would have particularly exciting consequences for the neutrinos belonging to extra generations. Particularly interesting is the mirror case, which forces the three mirror neutrinos to be heavy neutral leptons with masses around 50-100 GeV. They could even be the source [39] of the seesaw mechanism in which case, the mirror and ordinary families would be forced to mix by a tiny amount. Although this is not mandatory, these mixings are plausible and are naturally small enough (technically, the mirror symmetry preserves their smallness) to evade the Z width constraint. In all honesty, this appealing, simple and testable seesaw picture may not be very convincing. After all, one needs new physics to generate the Majorana masses of mirror neutrinos and there is no reason that the new physics is not generating Majorana masses for ordinary neutrinos, too.

What about the seesaw paradigm, with only one or two extra families? The former case is immediately ruled out since one predicts only one massive ordinary neutrino. In the latter case, one has an interesting prediction of maximally hierarchical neutrinos, since only two of them are massive. This fits nicely with cosmological considerations, which keep lowering the sum of light neutrino masses [40]. Moreover, the decays of the heavy extra neutrinos N are governed by the Dirac mass terms, which are functions of the leptonic mixing matrix, the masses of N 's and only one complex parameter [41]. This case can definitely be tested by measuring different flavor combinations of the final dilepton final states, similar to the minimal case of type I+III seesaw [42]. This could be an example of a testable seesaw mechanism at the LHC. If one gives up the dark matter candidate, EWPT work in the minimal setup with only the standard Higgs doublet, in which case the masses of N 's lie again between 50 GeV and 150 GeV.

In any case, irrespective of the seesaw, it is worth considering mirror symmetry not to be exact. Once N and E are produced pairwise, their decay can lead to the interesting two leptons and six jets events with no missing energy [43]. If N is of Majorana type, the characteristic feature is the equal decay rate in leptons and antileptons [44].

V. CONCLUSION AND OUTLOOK

In recent years, the inert scalar doublet model has become one of the popular extensions of the SM whose lightest component can play a role of the DM. Whereas its simplicity may be appealing, the inert nature is postulated by hand, which makes it more a model *for* rather than *of* dark matter. On the other hand, the inert nature is a natural scenario with the existence of mirror families, due to the electroweak precision constraints [3]. Mirror fermions have been suggested more than 50 years

ago, as a way of restoring parity, and are well motivated by a number of respected theoretical frameworks: KK compactification, $N = 2$ supersymmetry, family unification based on large orthogonal groups and some unified models of gravity.

This has encouraged us to carefully study the issue of dark matter in the context of the inert scalar doublet and mirror fermions. Since nothing in particular depends on the chirality of extra families, we have broadened our study by including the cases of only one and two extra families. The fourth generation has recently been the focus of a large body of research and as such deserves a special merit, in spite of the scalar's inertness not being called for. The case of two extra families does not possess any special features and thus we only commented on it in passing only. We now summarize the essential features case by case.

One extra family. It is not surprising that this case passes the EWPT since it works even with only one Higgs doublet as in the SM. For sufficiently light S and/or extra neutrino, the Higgs mass is excluded from the window 150–200 GeV by Tevatron data; otherwise the exclusion window is larger, 131–204 GeV [22]. As far as the direct DM detection is concerned, we find that the Xenon100 result restricts the DM mass to lie in the window $\frac{1}{2}m_h - 76$ GeV if the SM Higgs is light, and almost fixed at 74–76 GeV if the Higgs is heavy.

More extra families. Let us recall that since the extra quarks have to lie above the direct limits, their large Yukawa couplings rule out the light Higgs window because of vacuum stability [3]. It is then enough to consider a heavy Higgs $m_h \gtrsim 300$ –400 GeV. This is just above the Tevatron exclusion region which extends, in the case of three families, up to $m_h \gtrsim 240$ GeV. In terms of direct DM detection, the Xenon100 experiment together with the WMAP relic density constraint makes this scenario very predictive. In fact, the hadronic uncertainty in the h -nucleon coupling barely plays a role here, and the DM mass turns out to lie necessarily at 74–76 GeV. This could lead also to a characteristic signature in indirect DM search, in terms of the spectrum of particles resulting from both annihilation or decay from galactic haloes.

ACKNOWLEDGMENTS

The authors would like to thank BIAS for the inspiring and conducive research atmosphere. YZ would like to thank Kev Abazajian, Kaustubh Agashe, Zackaria Chacko, Rabi Mohapatra and Raman Sundrum for fruitful comments, and acknowledge hospitality from theoretical hadronic physics and elementary particles groups at University of Maryland during the final stage of this work.

Appendix A: Explicit formulæ for electroweak oblique parameters: Higgs sector

In the calculation of electroweak oblique parameters S , T and U for the Higgs sector, we apply the generic formulas given in [34] to the case with two Higgs doublets. The SM Higgs mass is denoted as m_h , while the reference point mass (corresponding to $S = T = U = 0$) is m_r , which is taken to be 120 GeV throughout the paper.

$$S_H = \frac{1}{24\pi} \left\{ (2s_W^2 - 1)^2 G(m_C^2, m_C^2, m_Z^2) + \ln \left(\frac{m_A^2 m_h^2 m_S^2}{m_C^4 m_r^2} \right) + \sin^2 \theta^2 G(m_A^2, m_h^2, m_Z^2) + \cos^2 \theta^2 G(m_A^2, m_S^2, m_Z^2) \right. \\ \left. + \sin^2 \theta^2 \hat{G}(m_S^2, m_Z^2) + \cos^2 \theta^2 \hat{G}(m_h^2, m_Z^2) - \hat{G}(m_r^2, m_Z^2) \right\}, \quad (\text{A1})$$

$$T_H = \frac{1}{16\pi M_W^2 s_W^2} \left\{ F(m_C^2, m_A^2) + \sin^2 \theta^2 [F(m_C^2, m_h^2) - F(m_A^2, m_h^2)] + \cos^2 \theta^2 [F(m_C^2, m_S^2) - F(m_A^2, m_S^2)] \right. \\ \left. + 3 \sin^2 \theta^2 [F(m_Z^2, m_S^2) - F(m_W^2, m_S^2)] + 3 \cos^2 \theta^2 [F(m_Z^2, m_h^2) - F(m_W^2, m_h^2)] - 3 [F(m_Z^2, m_r^2) - F(m_W^2, m_r^2)] \right\}, \quad (\text{A2})$$

$$U_H = \frac{1}{24\pi} \left\{ -(2s_W^2 - 1)^2 G(m_C^2, m_C^2, m_Z^2) + G(m_C^2, m_A^2, m_W^2) + \sin^2 \theta^2 [G(m_C^2, m_h^2, m_W^2) - G(m_A^2, m_h^2, m_Z^2)] \right. \\ \left. + \cos^2 \theta^2 [G(m_C^2, m_S^2, m_W^2) - G(m_A^2, m_S^2, m_Z^2)] + \sin^2 \theta^2 [\hat{G}(m_S^2, m_W^2) - \hat{G}(m_S^2, m_Z^2)] \right. \\ \left. + \cos^2 \theta^2 [\hat{G}(m_h^2, m_W^2) - \hat{G}(m_h^2, m_Z^2)] - [\hat{G}(m_r^2, m_W^2) - \hat{G}(m_r^2, m_Z^2)] \right\}, \quad (\text{A3})$$

where

$$G(x_1, x_2, x_3) = -\frac{16}{3} + 5 \frac{x_1 + x_2}{x_3} - 2 \frac{(x_1 - x_2)^2}{x_3^2} + \Delta \frac{f(x_1, x_2, x_3)}{x_3^3} + \frac{3}{x_3} \left(\frac{x_1^2 + x_2^2}{x_1 - x_2} - \frac{x_1^2 - x_2^2}{x_3} + \frac{(x_1 - x_2)^3}{3x_3^2} \right) \ln \frac{x_1}{x_2}, \quad (\text{A4})$$

$$f(x_1, x_2, x_3) = \begin{cases} \sqrt{\Delta} \ln \left| \frac{x_1 + x_2 - x_3 - \sqrt{\Delta}}{x_1 + x_2 - x_3 + \sqrt{\Delta}} \right| & \Delta > 0 \\ 2\sqrt{-\Delta} \left[\arctan \left(\frac{x_1 - x_2 + x_3}{\sqrt{-\Delta}} \right) - \arctan \left(\frac{x_1 - x_2 - x_3}{\sqrt{-\Delta}} \right) \right] & \Delta < 0 \end{cases}, \quad (\text{A5})$$

$$\Delta = x_3^2 - 2x_3(x_1 + x_2) + (x_1 - x_2)^2, \quad (\text{A6})$$

$$F(x_1, x_2) = \frac{x_1 + x_2}{2} - \frac{x_1 x_2}{x_1 - x_2} \ln \frac{x_1}{x_2}, \quad (\text{A7})$$

$$\hat{G}(x_1, x_2) = G(x_1, x_2, x_2) + 12 \left[-2 + \left(\frac{x_1 - x_2}{x_2} - \frac{x_1 + x_2}{x_1 - x_2} \right) \ln \frac{x_1}{x_2} + \frac{f(x_1, x_2, x_2)}{x_2} \right]. \quad (\text{A8})$$

-
- [1] E. Aprile *et al.* [XENON100 Collaboration], [arXiv:1104.2549 [astro-ph.CO]].
- [2] R. Barbieri, L.J. Hall, V.S. Rychkov, Phys. Rev. **D74** (2006) 015007 [hep-ph/0603188].
- [3] H. Martinez, A. Melfo, F. Nesti, G. Senjanovic, Phys. Rev. Lett. **106**, 191802 (2011). [arXiv:1101.3796 [hep-ph]].
- [4] H. -J. He, N. Polonsky, S. -f. Su, Phys. Rev. **D64**, 053004 (2001). [hep-ph/0102144].
- [5] E. Witten, Nucl. Phys. **B186** (1981) 412.
- [6] M. Gell-Mann, P. Ramond, R. Slansky, "Complex Spinors And Unified Theories"; F. Wilczek, A. Zee, Phys. Rev. **D25**, 553 (1982).
- [7] G. Senjanović, F. Wilczek, A. Zee, Phys. Lett. **B141** (1984) 389.

- [8] J. Bagger, S. Dimopoulos, Nucl. Phys. **B244** (1984) 247.
- [9] F. del Aguila, M. Dugan, B. Grinstein, L. J. Hall, G. G. Ross, P. C. West, Nucl. Phys. **B250** (1985) 225.
- [10] F. Nesti, R. Percacci, Phys. Rev. **D81**, 025010 (2010).
- [11] T. D. Lee, C. -N. Yang, Phys. Rev. **104** (1956) 254-258.
- [12] M. A. Shifman, A. I. Vainshtein, V. I. Zakharov, Phys. Lett. **B78** (1978) 443.
- [13] H. Flacher, M. Goebel, J. Haller, A. Hocker, K. Monig and J. Stelzer, Eur. Phys. J. C **60** (2009) 543 [[arXiv:0811.0009](#) [hep-ph]].
- [14] H. Murayama, V. Rentala, J. Shu, T. T. Yanagida, [[arXiv:1012.0338](#) [hep-ph]].
- [15] L. Lopez Honorez, E. Nezri, J.F. Oliver *et al.*, JCAP **0702** (2007) 028 [[hep-ph/0612275](#)]; T. Hambye, F.-S. Ling, L. Lopez Honorez *et al.*, JHEP **0907**, 090 (2009) [[arXiv:0903.4010](#)];
- [16] E.M. Dolle, S. Su, Phys. Rev. **D80** (2009) 055012 [[arXiv:0906.1609](#)].
- [17] A. Djouadi, J. Kalinowski, M. Spira, Comput. Phys. Commun. **108**, 56-74 (1998). [[hep-ph/9704448](#)].
- [18] G. D. Kribs, T. Plehn, M. Spannowsky and T. M. P. Tait, Phys. Rev. D **76**, 075016 (2007) [[arXiv:0706.3718](#) [hep-ph]].
- [19] J. S. Lee, A. Pilaftsis, M. S. Carena, S. Y. Choi, M. Drees, J. R. Ellis and C. E. M. Wagner, Comput. Phys. Commun. **156** (2004) 283 [[arXiv:hep-ph/0307377](#)].
- [20] A. Djouadi, Phys. Rept. **457**, 1 (2008) [[arXiv:hep-ph/0503172](#)].
- [21] E. Arik, O. Cakir, S. A. Cetin and S. Sultansoy, Phys. Rev. D **66**, 033003 (2002) [[arXiv:hep-ph/0203257](#)].
- [22] T. Aaltonen *et al.* [CDF and D0 Collaboration], [arXiv:1005.3216](#) [hep-ex].
- [23] J. Baglio, A. Djouadi, S. Ferrag and R. M. Godbole, [arXiv:1101.1832](#) [hep-ph].
- [24] W. -Y. Keung, P. Schwaller, [[arXiv:1103.3765](#) [hep-ph]].
- [25] H. S. Lee, Z. Liu and A. Soni, [arXiv:1105.3490](#) [hep-ph].
- [26] G. Belanger, F. Boudjema, A. Pukhov and A. Semenov, Comput. Phys. Commun. **176**, 367 (2007) [[arXiv:hep-ph/0607059](#)].
- [27] J. Dunkley *et al.* [WMAP Collaboration], Astrophys. J. Suppl. **180**, 306-329 (2009). [[arXiv:0803.0586](#) [astro-ph]]; K. Nakamura *et al.* [Particle Data Group Collaboration], J. Phys. G **G37**, 075021 (2010).
- [28] L. Lopez Honorez and C. E. Yaguna, JCAP **1101**, 002 (2011) [[arXiv:1011.1411](#) [hep-ph]].
- [29] L. Lopez Honorez and C. E. Yaguna, JHEP **1009**, 046 (2010) [[arXiv:1003.3125](#) [hep-ph]].
- [30] S. Andreas, T. Hambye and M. H. G. Tytgat, JCAP **0810**, 034 (2008) [[arXiv:0808.0255](#) [hep-ph]].
- [31] J. Giedt, A. W. Thomas and R. D. Young, Phys. Rev. Lett. **103**, 201802 (2009) [[arXiv:0907.4177](#) [hep-ph]].
- [32] J. R. Ellis, K. A. Olive and C. Savage, Phys. Rev. D **77**, 065026 (2008) [[arXiv:0801.3656](#) [hep-ph]].
- [33] P. Salucci, F. Nesti, G. Gentile, C. F. Martins, Astron. Astrophys. **523**, A83 (2010); M. Weber, W. de Boer, Astron. Astrophys. **509** (2010) A25.
- [34] W. Grimus, L. Lavoura, O. M. Ogreid and P. Osland, Nucl. Phys. B **801**, 81 (2008) [[arXiv:0802.4353](#) [hep-ph]].
- [35] A. A. Abdo *et al.*, Phys. Rev. Lett. **104**, 091302 (2010) [[arXiv:1001.4836](#) [astro-ph.HE]].
- [36] K. Ishiwata and M. B. Wise, Phys. Rev. D **83** (2011) 074015 [[arXiv:1103.0611](#) [hep-ph]].
- [37] E. Dolle, X. Miao, S. Su, B. Thomas, Phys. Rev. **D81**, 035003 (2010). [[arXiv:0909.3094](#) [hep-ph]]; X. Miao, S. Su, B. Thomas, Phys. Rev. **D82**, 035009 (2010). [[arXiv:1005.0090](#) [hep-ph]]; Q. H. Cao, E. Ma and G. Rajasekaran, Phys. Rev. D **76**, 095011 (2007) [[arXiv:0708.2939](#) [hep-ph]].
- [38] M. Kadastik, K. Kannike, A. Racioppi and M. Raidal, Phys. Lett. B **694**, 242 (2010) [[arXiv:0912.3797](#) [hep-ph]].
- [39] P. Q. Hung, Phys. Lett. **B649** (2007) 275-279. [[hep-ph/0612004](#)].
- [40] For a recent study, see S. Hannestad, A. Mirizzi, G. G. Raffelt and Y. Y. Y. Wong, JCAP **1008**, 001 (2010) [[arXiv:1004.0695](#) [astro-ph.CO]] and references therein.
- [41] A. Ibarra, G. G. Ross, Phys. Lett. **B591**, 285-296 (2004). [[hep-ph/0312138](#)].
- [42] B. Bajc, M. Nemevsek, G. Senjanović, Phys. Rev. **D76** (2007) 055011. [[hep-ph/0703080](#)]. A. Arhrib, B. Bajc, D. K. Ghosh, T. Han, G. -Y. Huang, I. Puljak, G. Senjanović, Phys. Rev. **D82** (2010) 053004. [[arXiv:0904.2390](#) [hep-ph]].
- [43] L. M. Carpenter, A. Rajaraman, D. Whiteson, [[arXiv:1010.1011](#) [hep-ph]].
- [44] W. -Y. Keung, G. Senjanović, Phys. Rev. Lett. **50** (1983) 1427. For a recent review and references, see e.g., G. Senjanović, [[arXiv:1012.4104](#) [hep-ph]]; [[arXiv:0911.0029](#) [hep-ph]].